Neutron Laue Diffraction Study on the Magnetic Phase Diagram of Multiferroic MnWO4 under Pulsed High Magnetic Fields

H. Nojiri

Publisher's version / Version de l'éditeur:
https://doi.org/10.1103/PhysRevLett.106.237202
Physical Review Letters, 106, 23, 2011-06-01

Neutron Laue Diffraction Study on the Magnetic Phase Diagram of Multiferroic $MnWO_4$ under Pulsed High Magnetic Fields

H. Nojiri,[1] S. Yoshii,[1] M. Yasui,[1] K. Okada,[1] M. Matsuda,[2] J.-S. Jung,[3] T. Kimura,[3] L. Santodonato,[4] G. E. Granroth,[4] K. A. Ross,[5] J. P. Carlo,[5] and B. D. Gaulin[5]

[1]*Institute for Materials Research, Tohoku University, Sendai 980-8577, Japan*
[2]*Quantum Beam Science Directorate, Japan Atomic Energy Agency (JAEA), Tokai, Ibaraki 319-1195, Japan*
[3]*Graduate School of Engineering Science, Osaka University, Osaka 560-8531, Japan*
[4]*Neutron Scattering Sciences Division, Oak Ridge National Laboratory, Oak Ridge, Tennessee*
[5]*Department of Physics and Astronomy, McMaster University, Hamilton, Ontario, L8S 4M1, Canada*

(Received 21 January 2011; published 8 June 2011)

We have combined time-of-flight neutron Laue diffraction and pulsed high magnetic fields at the Spallation Neutron Source to study the phase diagram of the multiferroic material $MnWO_4$. The control of the field-pulse timing enabled an exploration of magnetic Bragg scattering through the time dependence of both the neutron wavelength and the pulsed magnetic field. This allowed us to observe several magnetic Bragg peaks in different field-induced phases of $MnWO_4$ with a single instrument configuration. These phases were not previously amenable to neutron diffraction studies due to the large fields involved.

DOI: 10.1103/PhysRevLett.106.237202 PACS numbers: 75.25.−j, 61.05.F−, 75.85.+t

Neutron diffraction is an essential probe of magnetism in matter, which is routinely used to investigate diverse structures and phase diagrams in magnetic materials [1]. Geometrically frustrated magnets [2] and those possessing competing interactions may possess a complicated, macroscopically degenerate ground state. For such cases, application of a magnetic field may lift these degeneracies, revealing a nontrivial ground state. Couplings between spin, charge, orbital, and lattice degrees of freedom in materials can also compete and lead to rich phase behavior at low temperatures and at high magnetic fields. A specific example of topical interest is multiferroic phenomena, in which ferroelectricity is induced by a noncollinear magnetic structure [3]. The elucidation of the rich temperature-magnetic field phase diagrams of multiferroic materials is critical to their understanding, and new cutting edge capabilities for neutron diffraction in high magnetic fields are expected to yield important insights. In this Letter, we present the first application of neutron Laue diffraction combined with pulsed magnetic fields, using a white neutron beam at the Spallation Neutron Source (SNS) [4].

Conventional neutron diffraction studies can currently employ a maximum steady state magnetic field of 17 T, available at the Helmholtz Zentrum Berlin [5]. Recently, monochromatic neutron diffraction in a pulsed magnetic field up to 30 T was carried out using a reactor-based neutron source [6]. In that case, a continuous beam of monochromatic neutrons was employed and a single position in reciprocal space was investigated while the magnetic field was pulsed. Typically 100 to 200 field pulses are required at each $\boldsymbol{Q}$ point for adequate statistics. An advantage of this method is its ability to continuously monitor the field dependence of the peak diffracted intensity; however, the time required to conduct a survey of reciprocal space in this manner is logistically prohibitive.

To overcome these challenges, we combined a pulsed magnetic field with a pulsed white neutron beam, employing wavelength-resolved diffraction based on neutron time of flight (TOF) (some technical aspects of the method are discussed in a review article [7]). This method has several advantages. First, one obtains a higher neutron flux per magnetic field pulse since almost the whole flux is delivered within the short time that the field is applied to the sample. Second, the combination of a two-dimensional detector array and a wide bandwidth neutron beam enables a wide survey in reciprocal space without changing the instrument configuration. This Laue diffraction in high magnetic fields allows for efficient searches for unknown, field-induced magnetic Bragg peaks. Third, it is possible to perform a multidimensional measurement by time correlating the pulsed field with the arrival time of neutrons of differing wavelengths at the sample. A wide variety of field surveys are possible by using a variety of magnetic field-pulse shapes and relative field-neutron pulse delay times. These unique features of combining pulsed neutrons with pulsed magnetic fields should be very powerful in elucidating complex magnetic phase diagrams in new materials.

In the present work, a half-sinusoidal magnetic field-pulse is produced by a portable pulsed magnet system consisting of a mini-solenoid magnet, an insert for a ^{4}He ''orange cryostat'', and a capacitor bank. The bore of the magnet is 12 mm and provides a range of accessible scattering angles up to 30°. The configuration of the instrument is shown in Fig. 1(c) and is realized on the SEQUOIA spectrometer at the SNS operating in a white beam (~ 0.7 Å bandwidth) mode [8]. The magnet coil axis is set nearly parallel to the incident beam, and a forward

scattering geometry is used. Thus, the scattering vector, $\boldsymbol{Q}$, is nearly perpendicular to the magnetic field. The magnet is immersed in liquid N_2 and contained in an insert within the He cryostat. This allows for fast cooling of the magnet after each field pulse. The details of the insert are given elsewhere [6,9]. The energy of the capacitor bank is 6.3 kJ with 5.6 mF capacitance. A typical pulse width is 5 msec, which is 30% of the neutron pulse time-frame (17 msec), thus several Bragg peaks, corresponding to different TOFs, can be observed during a single field pulse. The field-pulse time delay is set by a timing controller with 0.25 μ sec precision. A maximum magnetic field of 30 T is generated every 5 min.

The experiment utilized event-based data collection, wherein all the neutron pulse frames, both in-field and zero-field, are collected and stored frame by frame. The frames are sorted into field-on and field-off groups. Each group is then summed to produce a field-on and a field-off TOF histogram of the neutron counts per detector pixel. Cross-correlation of the magnetic field-pulse timing with each TOF bin of the histogram gives the magnetic field for each TOF bin. Furthermore, the field for a given TOF bin can be varied by shifting the delay of the field pulses relative to the timing of the neutron pulses.

We studied the multiferroic material $MnWO_4$ which crystalizes into a monoclinic space group $P2/c$ with lattice parameters $a = 4.8226(3)$ Å, $b = 5.7533(6)$ Å, $c = 4.9923(5)$ Å and $\beta = 91.075(7)°$ [10]. $MnWO_4$ is a typical multiferroic system [11], showing a coexistence of magnetic and ferroelectric (FE) orderings. Such phenomena have been theoretically discussed, for example, in terms of the spin current model [12], wherein the breaking of inversion symmetry in a noncollinear magnetic structure results in a ferroelectric polarization (P). Hence, the determination of the magnetic structure is crucial to understanding multiferroics. As shown in Fig. 2(b), $MnWO_4$ consists of zig-zag chains of Mn^{2+} ($S = 5/2$) ions along the c-axis. Frustration results from competition between nearest- and next-nearest-neighbor exchange interactions along the chains. Figure 2(a) summarizes the magnetic phase diagram with a magnetic field applied along the magnetic easy axis, as determined by P measurements [13]. In zero magnetic field, the AF1, AF2, and AF3 phases are known to be a commensurate (C) collinear phase with $\boldsymbol{Q}_C = (\pm\frac{1}{4}, \frac{1}{2}, \frac{1}{2})$, an incommensurate (IC) cycloidal phase with $\boldsymbol{Q}_{\rm IC} = (-0.214, \frac{1}{2}, 0.457)$, and an IC collinear phase with the identical $\boldsymbol{Q}_{\rm IC}$ as AF2, respectively [10]. The spin arrangements of the AF1 and AF2 phases are depicted in Fig. 2(b). Only the noncollinear AF2 phase exhibits a FE polarization.

In high magnetic fields, there are at least two ordered phases with unknown structures, HF and IV. Furthermore, a distinct memory effect is observed in-field-dependent measurements that follow the path AF1⇄AF2⇄HF⇄IV through the phase diagram [13,14]. Namely, the AF2 and IV phases always show opposite polarizations relative to each other, irrespective of the direction of the initial polarization. This occurs even when the magnetic field scan path traverses the nonpolar ($P = 0$) HF phase. Small IC phase domains in the nonpolar phase have been proposed as a cause of the memory effect [14]. Such domains could seed the polarization in the reentrant transition. To clarify the mechanism of the multiferroic behavior and the distinct memory effect in $MnWO_4$, the magnetic structures in the high field phases need to be understood. For the HF phase, a commensurate spin flop structure has been proposed by conventional neutron diffraction at 14.5 T [15]. However, only commensurate Bragg reflections were studied.

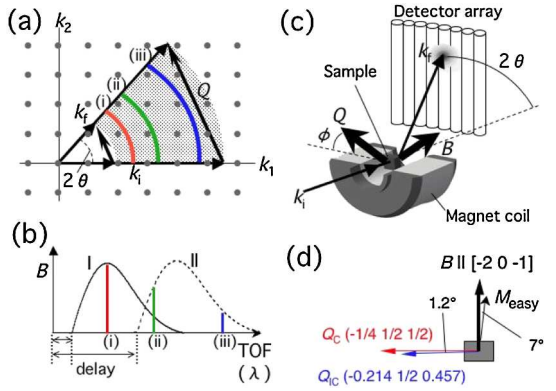

FIG. 1 (color online). (a) Reciprocal space map showing Bragg diffraction in the Laue method. The shaded area can be simultaneously captured, and circular arcs correspond to constant field line in a pulsed field. (b) An example of the delay time control for half-sinusoidal field pulses. The start time of field-pulse I (solid line) is set so that the maximum field coincides with the TOF (i) in (a). In the case II (dashed line), two reflections at (ii) and (iii) can be observed in a single field-pulse time-frame. (c) Schematic cut-away view of the magnet coil and the experimental arrangement. (d) The configuration of magnetic field B, and scattering vectors $\boldsymbol{Q}_C$ and $\boldsymbol{Q}_{\rm IC}$.

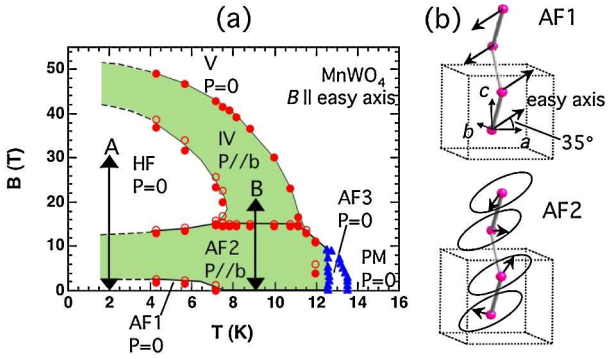

FIG. 2 (color online). (a) The magnetic phase diagram of $MnWO_4$ for B parallel to magnetic easy axis [13]. Ferroelectric phases are shaded in green. The present experiment has been performed along the arrows A and B. (b) A schematic diagram of the magnetic structures in the AF1 and AF2 phases. In AF1, the magnetic easy axis lies in the ac plane and is tilted by 35° from the a axis.

In order to access both the $\boldsymbol{Q}_C$ and $\boldsymbol{Q}_{\mathrm{IC}}$ reflections while simultaneously applying a magnetic field aligned close to the easy axis, we employed a scattering geometry as shown in Fig. 1(d). The magnetic field was applied along [2,0,1], which deviates by 7° from the magnetic easy axis [10,11]. The phase diagram is known to be insensitive to small deviations in the field alignment [16]. Figure 3(a) shows the time integrated Laue images at $B = 0$ T, where the horizontal and the vertical axes are along the $(-h,2h,2h)$ and $(2k,0,k)$ directions, respectively. At $T = 2$ K in the AF1 phase, Bragg scattering appears at $h = \frac{1}{4}$ and $k = 0$ position corresponding to $\boldsymbol{Q}_C = (-\frac{1}{4}, \frac{1}{2}, \frac{1}{2})$, while, at 9 K in the AF2 phase, scattering is observed at the $h = 0.23$ and $k = 0.0035$ position corresponding to $\boldsymbol{Q}_{\mathrm{IC}} = (-0.214, \frac{1}{2}, 0.457)$. The C and IC peaks are easily distinguished as their d spacings differ by 0.45 Å. This results in a TOF difference of 2.3 msec, and thus the $\boldsymbol{Q}_C$ (AF1) and $\boldsymbol{Q}_{\mathrm{IC}}$ (AF2) reflections appears at 9.1 and at 11.4 msec, respectively. By adjusting the delay of the $B_{\max} = 25$ T magnetic field pulse, the C and IC Bragg reflections are detected within one neutron frame but at different TOF values at 2 K. In Fig. 3(b) a TOF spectrum, integrated over the appropriate detector pixels, is plotted together with the waveform of the pulsed magnetic field, which initiates 7.6 msec after the neutron pulse is generated. The TOF spectrum is obtained by accumulating 100–150 magnetic field pulses. Two TOF ranges that correspond to times where the magnetic field puts the sample in the AF2 phase are shaded in green. The latter range covers the TOF of the IC Bragg reflection, and corresponds to a magnetic field ~4 T. Near the peak field, the C reflection is observed, which indicates that the magnetic structure of the HF phase is commensurate with the wave vector of $\boldsymbol{Q}_C = (-\frac{1}{4}, \frac{1}{2}, \frac{1}{2})$. We observe that the C peak is much broader than the IC peak, and that it displays a small splitting. The origin of the splitting will be discussed later.

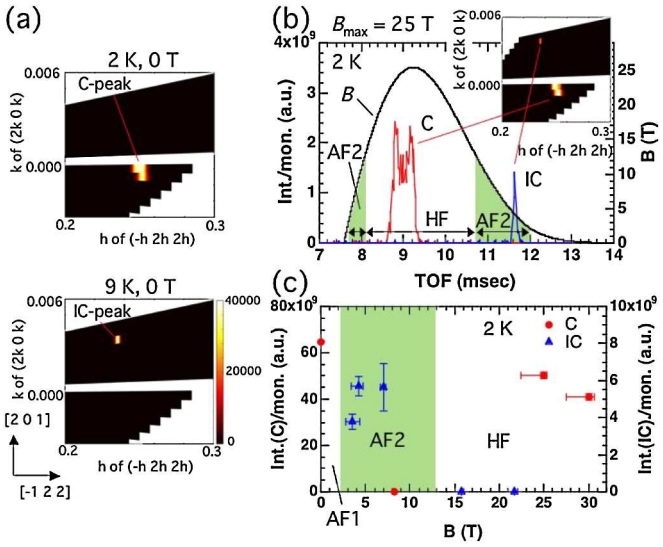

FIG. 3 (color online). (a) Color contour map of Laue diffraction spanned by $[-1,2,2]$ and $[2,0,1]$ axes in reciprocal space and taken at $B = 0$ T. The C and IC peaks are observed at 2 K and 9 K, respectively. (b) The pixel-integrated TOF spectrum at 2 K with $B_{\max} = 25$ T. Scattering from the C and IC positions are in red and blue, respectively. Inset: time integrated Laue diffraction shows the simultaneous measurement of the C and IC reflections. (c) The magnetic field dependence of integrated C and IC Bragg intensities at 2 K.

The magnetic field dependence of the intensities of the C and IC Bragg reflections at 2 K are obtained by using magnet delay times that maximize the fields at the C and IC peaks independently. Within our wide angular observation range, only the C and IC reflections appear at 2 K up to 30 T. Figure 3(c) summarizes the field variation of the integrated intensity for the two peaks. It clearly shows that the C reflection disappears in the AF2 phase and reappears in the HF phase. Our results further clarify that the IC reflection exists only in the AF2 phase, and a residual IC component does not appear in HF phase. These measurements place an upper limit of $<0.1\%$ on the possible IC domain volume at 22 T. Hence, in practical terms, our results negate the hypothesis that a small remnant of IC domain in the HF phase causes memory effect.

The intensity of the C reflection at 30 T is reduced by 30% from the zero-field value. This change could be due to a decrease of the antiferromagnetic structure factor, or to a change of the orientational factor in the cross section. In the collinear structure at 0 T, the reduction of the orientational factor is small because the Q is nearly perpendicular to the magnetic moments. After a spin flop transition, the moment is expected to be perpendicular to the easy axis and the magnetic moments can have both parallel and perpendicular components relative to the Q. The branching ratio into two components depends on the anisotropy in the plane normal to the easy axis. It is easily derived that the magnetic structure factor becomes zero for the parallel component. On the other hand, an intensity reduction of 25% is expected by structure factor calculation for perpendicular components considering that the uniform magnetization at 30 T is about $1/2$ of the saturation magnetization. These considerations suggest that the magnetic moments lie in the plane nearly orthogonal to the Q in the HF phase.

We next discuss the magnetic field dependence of the small splitting observed in the C reflection within the HF and AF1 phases. Figure 4(a) shows a detailed view of the time-integrated Laue images of the C reflection in the AF1 and HF phases. At 0 T, the intensity is distributed evenly along the vertical $(2k,0,k)$ direction. In the HF phase, the intensity shifts to more negative k values and the distribution is much suppressed. At 0 T and in area A (which is the signal in one PSD), the peak consists of two components with a difference in d spacing of 1.4%. In area B (the signal in the adjacent PSD), the lower d-spacing component is dominant. The ratio of the two components changes in the HF phase, showing an enhancement of the lower d-spacing component. We also note that the change is reproducible among different magnetic field sweeps.

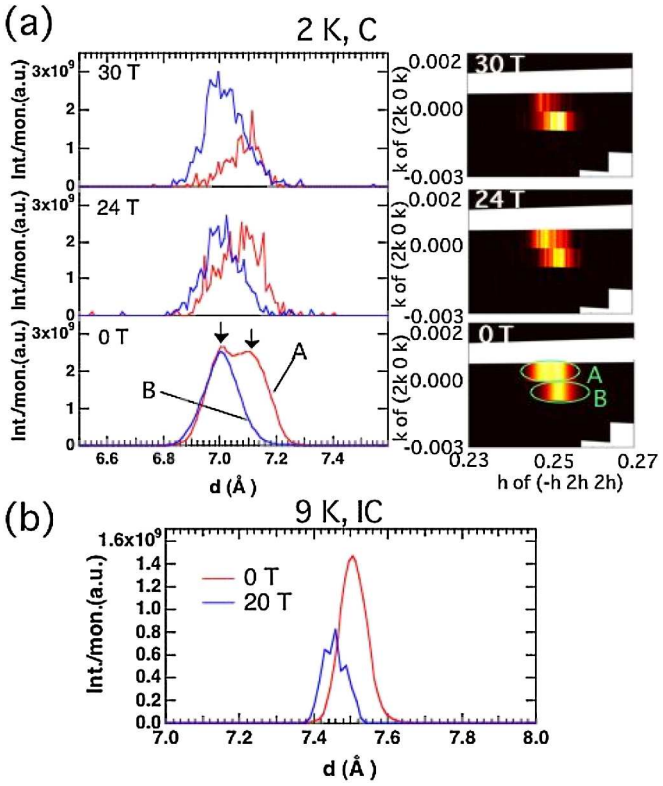

FIG. 4 (color online). (a) The right panels show magnified Laue images around the $\boldsymbol{Q}_C$ position within the AF1 and HF phases. The left panels show the TOF spectrum with the x axis converted to d spacing. The red and blue lines depict intensity as a function of d at the A and B areas, respectively, of the Laue image in the bottom right panel. (b) The TOF spectrum for IC reflections in AF2 (red line) and IV (blue line) phases. The x axis has been converted to d spacing.

As for an origin of the splitting of the C reflection, a modification of the crystal lattice is unlikely. Absence of a splitting in the IC reflection at 0 T [Fig. 4(b)] excludes a twinned domain in the monoclinic crystal structure. The absence of a splitting in the nuclear reflections such as $(h,0,2h)$ are inconsistent with a lowering of the crystal symmetry to triclinic. A possible cause, on the other hand, is a magnetic origin, such as an IC modulation of the magnetic structure around $(-\frac{1}{4}, \frac{1}{2}, \frac{1}{2})$. Since the splitting is as small as 1.4% in d spacing, the modulation pitch would have to be very long. Such long modulations have been sometimes observed in multiferroic systems, such as $BiFeO_3$ [17]. Whatever its cause, we suggest that the observed splitting may be related to the memory effect in $MnWO_4$.

We have also examined phase IV at 9 K and found that the IC reflection alone is observed at 20 T [Fig. 4(b)]. The magnetic wave vector at 20 T is nearly the same as that of the AF2 phase at 0 T and at 9 K. We determine the IC wave vector in phase IV to be $(-0.215, 0.503, 0.460)$, very close to $\boldsymbol{Q}_{\mathrm{IC}} = (-0.214, \frac{1}{2}, 0.457)$ in the AF2 phase. This is the first direct determination of the IC wave vector in phase IV. Since the strong magnetic field favors a flop of the spiral spin plane [18], it is plausible that the spins rotate within the plane that is normal to the field (easy) direction in phase IV. Indeed, according to structure factor considerations, this flop of the spiral plane explains very well the considerable reduction of the IC reflection intensity observed in phase IV (nearly half that within the AF2 phase). It is also worth noting that a theoretical model predicts FE polarization that is parallel to the b axis for the flopped spiral structure [12,19], which agrees with the polarization measurement in phase IV [13]. Thus our neutron study suggests a noncollinear spiral structure for phase IV.

In conclusion, we have demonstrated a breakthrough in magnetic neutron diffraction at high magnetic fields by combining pulsed magnetic fields with time resolved neutron Laue diffraction. This new technique allowed us to explore and clarify the nature of the magnetic structures of two high field phases, HF and IV, of the multiferroic $MnWO_4$.

We thank A. Parizzi, J. Kohl, P. Peterson, A. Kolenikov, and T. Sherline for invaluable technical assistance with the experiment. This work was supported by the Priority Areas "High Field Spin Science in 100 T" (No. 451), and by the ICC-IMR Center and by GCOE-materials integration of Tohoku University. Work at McMaster University was supported by NSERC. This research at ORNL's SNS, was sponsored by the Scientific User Facilities Division, Office of Basic Energy Sciences, U. S. Department of Energy.

[1] *Methods of Experimental Physics*, edited by K. Skold and D. L. Price (Academic, New York, 1986), Vol. 23.
[2] *Frustrated Spin Systems*, edited by H. T. Diep (World Scientific, Singapore, 2004).
[3] T. Kimura, Annu. Rev. Mater. Res. **37**, 387 (2007).
[4] T. E. Mason *et al.*, Physica (Amsterdam) **385–386B**, 955 (2006).
[5] M. Meissner and P. Smeibidl, Neutron News **12**, 12 (2001).
[6] S. Yoshii *et al.*, Phys. Rev. Lett. **103**, 077203 (2009).
[7] V. V. Nietz, Crystallogr. Rep. (Transl. Kristallografiya) **53**, 526 (2008), and references therein.
[8] G. E. Granroth *et al.*, J. Phys. Conf. Ser. **251**, 012058 (2010).
[9] H. Nojiri *et al.*, ILL Annual Report, p. 20 (2009).
[10] G. Lautenschläger *et al.*, Phys. Rev. B **48**, 6087 (1993).
[11] K. Taniguchi *et al.*, Phys. Rev. Lett. **97**, 097203 (2006).
[12] H. Katsura, N. Nagaosa, and A. V. Balatsky, Phys. Rev. Lett. **95**, 057205 (2005).
[13] H. Mitamura *et al.*, J. Phys. Conf. Ser. **150**, 042126 (2009).
[14] K. Taniguchi *et al.*, Phys. Rev. Lett. **102**, 147201 (2009).
[15] H. Ehrenberg *et al.*, Physica (Amsterdam) **276–278B**, 644 (2000).
[16] H. Ehrenberg *et al.*, J. Phys. Condens. Matter **9**, 3189 (1997).
[17] I. Sosnowska *et al.*, J. Phys. C **15**, 4835 (1982).
[18] T. Nagamiya *et al.*, Prog. Theor. Phys. **27**, 1253 (1962).
[19] M. Mostovoy, Phys. Rev. Lett. **96**, 067601 (2006).